JOURNAL OF GEOPHYSICAL RESEARCH, VOL. 100, NO. D6, PAGES 11,105–11,111, JUNE 20, 1995

Comparison of stratospheric temperatures from several lidars, using National Meteorological Center and microwave limb sounder data as transfer references

J. D. Wild,[1] M. E. Gelman,[2] A. J. Miller,[2] M. L. Chanin,[3] A. Hauchecorne,[3] P. Keckhut,[3] R. Farley,[4] P. D. Dao,[4] J. W. Meriwether,[4,5] G. P. Gobbi,[6] F. Congeduti,[6] A. Adriani,[6] I. S. McDermid,[7] T. J. McGee,[8] E. F. Fishbein[9]

Abstract. Stratospheric temperatures derived from five different lidars are compared. Although the lidars are in five separate geographic locations, the evaluation is accomplished by comparing each of the sets of lidar data taken over the course of a year (1991–1992) with temperatures interpolated to each location from daily global temperature analyses from the National Meteorological Center (NMC). Average differences between the lidars and NMC temperatures vary for the different lidars by up to 6.7 K. Part of this large average temperature difference is shown to be due to the real temperature variation throughout the day, and the different times of observation of the NMC data and each of the lidar systems. Microwave limb sounder (MLS) data from the upper atmosphere research satellite are used to model the diurnal and semidiurnal variations in temperature for each lidar location, for each season. After adjusting for the temperature changes caused by variations in observation time, average temperature differences are reduced among four of the five lidars, compared with the NMC temperatures, but still vary by as much as 3.9 K at stratospheric altitudes between 30 and 45 km. Results of direct comparisons at two permanent lidar sites with a mobile lidar show that sometimes agreement within 1 to 2 K is achieved, but for other cases, larger average differences are seen. Since the precision of lidar temperatures has been estimated to be better than 1 K, further research is needed to reconcile this small expected error with the larger average differences deduced here using measurements made under operational conditions.

Introduction

Stratospheric temperatures derived from lidar measurements have developed into an important source of information for many applications. Since details of Rayleigh lidar theory used to extract temperatures for the stratosphere and mesosphere can be found elsewhere [*Measures*, 1984], only an overview will be given here.

The Rayleigh lidar sends a pulse of monochromatic laser light into the atmosphere and measures the return signal with a detector placed at the ground. The time structure of the return yields the altitude of atmospheric scattering layers. If Mie scattering from aerosols is negligible, the number of elastically scattered photons is proportional to the product of the square of the atmospheric transmission of light from the lidar altitude to the scattering altitude, the molecular cross section for Rayleigh scattering, the molecular density at the scattering layer, and range-squared corrections. The constant of proportionality depends on the optical efficiency of the lidar and is independent of scattering altitude. If the atmospheric transmission is constant with altitude, or its altitude dependence is known, the proportionality relation can be inverted to give the relative molecular density as a function of altitude in terms of measured quantities. The assumption that the atmosphere is an ideal gas in hydrostatic equilibrium is used to extract the temperature profile from the relative density. *Keckhut et al.* [1993] give a detailed analysis of the impact on the resultant temperature of these assumptions, photon noise, and other factors, and find that in the stratosphere above the aerosol layer, temperatures determined from lidar measurements can be accurate to 1 K. Within an aerosol layer, temperatures from Rayleigh lidar can be up to 10 K too low [*Hauchecorne and Chanin*, 1980].

The lidar data used in this study were taken from the upper atmosphere research satellite (UARS) correlative program. Table 1 shows the names and locations of the various lidars, principal investigators for each site, the dates over which the

[1]Research and Data Systems Corporation, Greenbelt Maryland.
[2]Climate Analysis Center, National Meteorological Center, National Weather Service, National Oceanic and Atmospheric Administration, Washington, D.C.
[3]Service d'Aeronomie du Centre National de la Recherche Scientifique, Verrieres le Buisson, France.
[4]Air Force Phillips Laboratory, Geophysics Directorate, Hanscom Air Force Base, Bedford, Massachusetts.
[5]Now at Department of Physics and Astronomy, University of Clemson, Clemson, South Carolina.
[6]Istituto di Fisica dell'Atmosfera, Consiglio Nazionale delle Ricerche, Frascati, Italy.
[7]Jet Propulsion Laboratory, Table Mountain Facility, Wrightwood, California.
[8]Laboratory for Atmospheres, NASA Goddard Space Flight Center, Greenbelt, Maryland.
[9]Jet Propulsion Laboratory, California Institute of Technology, Pasadena.

Copyright 1995 by the American Geophysical Union.

Paper number 95JD00631.
0148-0227/95/95JD-00631$05.00

Table 1. Sites and Dates of Lidar Data

Site	Latitude	Longitude	Dates	Investigator	Points
TMO	34°N	118°W	Sept. 12, 1991 to Sept. 10, 1992	McDermid	126
HAN	42°N	71°W	Oct. 5, 1991 to Sept. 30, 1992	Farley, Dao	26
OHP	44°N	6°E	Oct. 30, 1991 to Sept. 14, 1992	Chanin, Hauchecorne, Keckhut	115
CEL	44°N	1°W	Oct. 2, 1991 to Sept. 16, 1992	Chanin, Hauchecorne, Keckhut	71
FRA	42°N	13°E	Sept. 19, 1991 to Sept. 10, 1992	Gobbi, Congeduti, Adriani	91
TMO	34°N	118°W	Feb. 19 to March 19, 1992	McGee	19
	34°N	118°W	Feb. 19 to March 19, 1992	McDermid	16
OHP	44°N	6°E	July 13 to Aug. 17, 1992	McGee	23
	44°N	6°E	July 13 to Aug. 17, 1992	Chanin, Hauchecorne, Keckhut	22

data have been used in this study, and the number of nights during the study period for which lidar measurements were made [*McDermid*, 1987; *Dao et al.*, 1989, 1990; *Hauchecorne et al.*, 1991; *Adriani, et al.*, 1991; *Ferrare et al.*, this issue; *McGee et al.*, 1992]. As Table 1 indicates, all sites are located in the northern hemisphere midlatitudes. The first five items, Table Mountain Observatory (TMO) in California, Hanscom Air Force Base (HAN) in Massachusetts, Observatoire d'Haute Provence (OHP) in France, Centre d'Etudes des Landes (CEL) in France, and Frascati (FRA) in Italy, correspond to long-term studies, of which we use approximately one full year of data. The final four items in Table 1 comprise two sets of at-sitc intercomparison investigations with McGee's mobile lidar.

Several of the investigations in Table 1, namely, OHP, CEL, TMO, and McGee, are also parts of the Network for the Detection of Stratospheric Change (NDSC) [*Kurylo and Solomon*, 1990]. The NDSC is a group of five globally located ground stations, several secondary stations, and satellite instruments measuring stratospheric temperature, ozone, and other chemical constituents. Dedicated to the purpose of long-term stratospheric monitoring, the NDSC focuses on long-term, high-quality data sets.

Although each of the lidar systems in Table 1 uses the same basic principles to derive the atmospheric temperature, the systems differ in detail. Table 2 contains pertinent information about the lidar systems under study [*McCormick*, 1993; *Keckhut et al.*, 1993; *McGee et al.*, 1992].

Four of the systems (HAN, OHP, CEL, and FRA) use lasers with wavelength 532 nm for which the atmospheric transmission is approximately constant for the altitudes of interest. In these cases, knowledge of the atmospheric transmission is not required for the derivation of the temperature profile that depends on the relative, not the absolute, density. The remaining experiments (TMO and McGee), however, use wavelengths near 350 nm for which the atmospheric transmission varies by as much as 1.5% [*Ferrare et al.*, this issue]. In these cases the altitude dependent atmospheric transmission is calculated to assure accurate temperature profiles. Since the atmospheric transmission varies with the density, a self-consistent determination of the density requires an iterative approach. Lidars using the 532-nm wavelength are more sensitive to aerosols than those using wavelengths near 350 nm.

The magnitude of the return signal depends on the product of the power of the laser, the detector area, and, for Rayleigh scattering, $1/\lambda^4$, where λ is the wavelength of the laser. Thus the power-aperture product determines the maximum altitude for which temperatures can be measured with a given precision for lasers of similar wavelengths. The lidars in this study use a variety of receivers, pulse rates, and pulse energies, resulting in power-aperture products ranging from 2 to 12.5 m^2 W. One should multiply the power-aperture product of the 353-nm lasers by 5.2 ($= \lambda_{532}^4/\lambda_{353}^4$) to compare with those of the 532-nm lidars. Thus the TMO lidar is the most powerful lidar in this study. Temperature profiles are measured to at least 70 km for all systems. The altitude range of this study (30–50 km) is well below this limit; thus, no deterioration of lidar data quality is expected at the top study levels for any of the lidar systems.

With the exception of the Hanscom system, the reported precision of the Rayleigh lidars, based on photon counting statistics, is usually less than 1 K for the 30- to 50-km range (see Table 2). The Frascati lidar occasionally reports a

Table 2. Lidar Instrument Details

	TMO	HAN	OHP	CEL	FRA	TMO-MCG	OHP-MCG
Laser λ, nm	H_2-SRS 353	Nd:YAG 532	Nd:YAG 532	Nd:YAG 532	Nd:YAG 532	XeF 351	XeF 351
Pulse rate, Hz	150	10	50	30	10	70	70
Energy/pulse, mJ	100	300	350	200	250	150	150
Receiver area, m^2	0.64	0.65	0.5	1.1	5.0 above 40 km; 0.2 below 40 km	0.45	0.45
Power-aperture product, m^2 W	9.6	2.0	8.8	6.6	12.5 above 40 km; 0.5 below 40 km	4.8	4.8
Altitude range, km	30–80	35–70	30–90	30–85	30–90	30–70	27–75
Integration time, hours	~2	~1–2	~1	~1	~2–4	~4–5	~3–4
Data resolution, km	0.6	0.3	0.3	0.3	0.3	0.15	0.15
Reported precision in 30- to 50-km range,* K	<1	1–3	<1 for 35–45 km; <1.5 elsewhere	<1 for 35–45 km; <1.5 elsewhere	<1.5 near 40 km; <1 elsewhere	<1	<1 Rayleigh; <10 Raman

*The precision is based on photon counting statistics.

precision of up to 1.5 K near 40 km, and the CEL and OHP lidars occasionally report the precision as high as 1.5 K for temperatures below 35 km and above 45 km. These occurrences are rare.

For the data presented in Table 2 the integration time varies from 1 to 5 hours. Coarse range resolution and long integration times serve to improve the instrument precision and to smooth time dependent features, e.g., gravity waves, of the profile. In the 30- to 50-km range of interest, gravity waves are generally less than 1 K in magnitude, so different integration times among the compared instruments will contribute to no more than 1 K of interinstrumental bias.

In the post-Pinatubo period under consideration, aerosols near 30 km degrade the accuracy of the Rayleigh lidar results. The McGee lidar at OHP uses the Raman shifted return at 382 nm to determine the temperature profile at 27–33 km. The Raman technique is similar to the Rayleigh technique except that the detector measures inelastically scattered light at the shifted wavelength. The advantage of this technique is that the return is not contaminated by the elastic scattering of aerosols; however, it may be somewhat attenuated by aerosols. Though the Raman technique is inherently less sensitive to aerosols than the Rayleigh technique, and thus a more direct measurement of molecular density, it cannot be used for high-altitude profiles because the return signal is weak compared with background noise. The large errors reported in McGee's OHP data set at low altitudes reflect the poor signal-to-noise ratio. The Hanscom lidar also has the capability of measuring the temperature profile for low altitudes with a Raman system [*Dao et al.*, 1990], but the September 1991 to September 1992 data set does not include data for these altitudes. At OHP, temperature measurements using vibrational Raman lidar have been made since 1988 [*Keckhut et al.*, 1990], though are not included in the September 1991 to September 1992 high-aerosol post-Pinatubo period. Measurements using a technique based on rotational Raman scattering eliminate both aerosol scattering and extinction, and will soon be operational at OHP [*Nedeljkovic et al.*, 1993; *Hauchecorne et al.*, 1992].

A principal impetus for this study is the evaluation of the expected errors for lidar data that we use to compare with National Meteorological Center (NMC) temperatures [*Finger et al.*, 1993]. NMC global stratospheric temperature analyses have been produced operationally since 1978. They are based on measurements of upwelling atmospheric and terrestrial radiation by the NOAA polar orbiting operational satellites. The satellites contain three multichannel instruments, the high-resolution infrared sounder (HIRS), the microwave sounding unit (MSU), and the stratospheric sounding unit (SSU), which together form the TIROS operational vertical sounder (TOVS). Each of the 27 channels senses a different altitudinal slice of the atmosphere as determined by the channel's weighting function. The scalar product of a temperature profile and a channel's weighting function yields the radiance as measured by that channel. The inverse problem of retrieving the temperature profile from a set of radiances is performed by the National Environmental Satellite and Data Information Service (NESDIS) via a minimum-variance algorithm, details of which can be found in the works by *Fleming et al.* [1986, 1988] and *Goldberg et al.* [1988].

NMC produces analyzed temperature maps for both the northern and southern hemispheres on a 65 × 65 polar-stereographic grid for 18 standard pressure levels from 1000 to 0.4 mbar. In the stratosphere (70, 50, 30, 10, 5, 2, 1, and 0.4 mbar, or approximately 18, 20, 24, 30, 35, 42, 48, and 55 km) a Cressman analysis is performed [*Finger et al.*, 1965; *Cressman*, 1959] using retrieved TOVS profiles gathered during the day from 0600 to 1800 UT. Archived day-minus-1 analyses are used for the initial guess map. For levels 70–10 mbar in the northern hemisphere, a second analysis is performed using the TOVS results as first guess and radiosonde 1200 UT data for the averaging process.

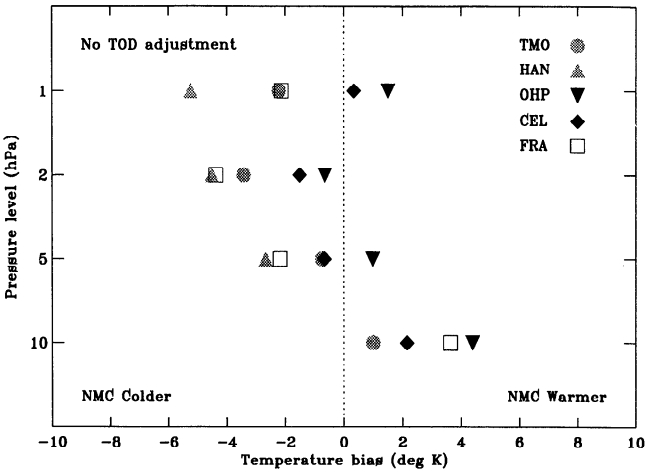

Figure 1. Average stratospheric temperature differences, NMC minus lidar, for several sites as described in Table 1. The standard estimate of error is discussed in text.

Because radiosonde data are not available for the analyses at the top four pressure levels (5–0.4 mbar), abrupt changes have been known to occur in the daily archive upon the change of operational satellite [*Finger et al.*, 1993]. Rocketsonde data are used to evaluate long-term stratospheric temperature measurements made by successive operational meteorological satellites, and to eliminate such shifts [*Gelman et al.*, 1986]. In recent years the number of rocketsonde observations has drastically diminished, compromising the validity of the results. Lidar data have been proposed as a substitute for rocketsonde data for this evaluation.

Comparisons of Lidar and NMC Temperatures

Figure 1 shows the average differences between NMC temperatures and lidar temperatures for each site, at pressure levels 10, 5, 2, and 1 mbar (30–45 km). NMC temperatures have been interpolated from the 65 × 65 grid to the lidar site. NMC heights for each pressure level provide the pressure-height relationship required to interpolate altitude-based lidar data to pressure level. The 95% confidence limit, or twice the standard error, for each average difference is from 0.5 to 2 K. Ideally, all calculated average difference values from the various stations would agree to within the confidence limits of the calculations. Such consistency among lidar results would indicate a uniform bias between all lidar measurements and NMC temperatures. Unfortunately, this is not the case. We see a spread in the average lidar temperature differences ranging from 3.4 K at 10 mbar to 6.7 K at 1 mbar.

We further note that the results are approximately

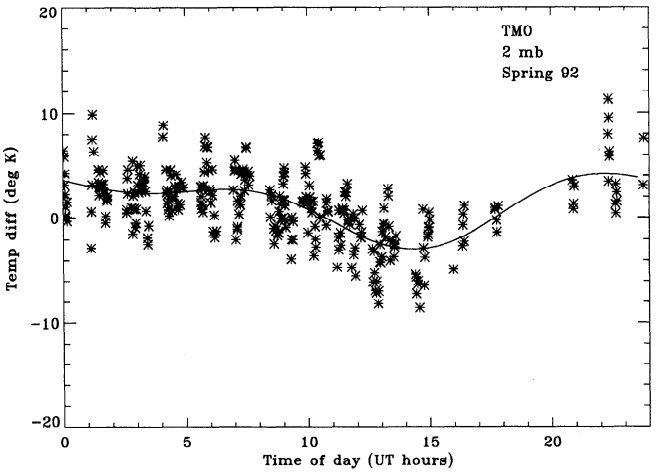

Figure 2. MLS-minus-NMC temperature differences as a function of time of day for Table Mountain Observatory at 2 mbar in the spring of 1992. Solid curve is fitted diurnal and semidiurnal variation as described in text.

grouped by eastern or western hemisphere. The U.S. station averages (shaded triangle and shaded circle) are consistently 1–5 K to the left of the French station averages (solid diamond and solid triangle). The Italian points at Frascati (open square), however, lie within the U.S. cluster for pressure levels 5, 2 and 1 mbar, but between the French locations for 10 mbar. The CEL and OHP averages have very much the same shape with respect to altitude, as one would expect, since the sites are within 600 km of each other and the instruments are operated by the same teams. However, there remains a bias of 1–2 K at all levels. This bias has also been noted in long-term (1986–1991) data sets from these sites [*Finger et al.*, 1993].

The results shown in Figure 1 do not include any consideration of the time of day at which the data are taken. The NMC stratospheric analyses for the 1991–1992 period are derived from NOAA 11 polar orbiting, sun-synchronous satellite measurements. NOAA 11 crosses the equator twice during each orbit, ascending over the equator at about 1530 and descending at about 0330 LT, with the local times at other geographical locations differing from these nominal times, depending on the distance from the equatorial crossing site. The 1200 UT NMC temperature analysis uses 12 hours of NOAA 11 data gathered between 0600 and 1800 UT that corresponds to ascending and descending data from six or seven orbits. Thus global comparisons of NMC and lidar data may be affected by average temperature differences expected between the hours of about 0330 LT (over the United States) and 1530 LT (over Europe). In addition, though lidar data are generally taken at night, the measurements occur at times varying between sunset and sunrise, thus introducing the further possibility of real differences in average temperature due to the time of data gathering between lidar and satellite. Studies that have estimated the magnitude of average temperature changes throughout the day have concluded that the diurnal and semidiurnal temperature changes range up to several degrees Kelvin, the magnitude varying significantly with height, season, and geographic location [*Dudhia et al.*, 1993; *Gille et al.*, 1991].

Data from the microwave limb sounder (MLS) on the UARS [*Waters*, 1993] may be used to estimate the regular variations of temperature with time throughout the day. Because the UARS satellite is not in a sun-synchronous orbit, profiles taken at a single geographic location on successive days and weeks are made at varying times throughout the day. The data span a full 24 hours in about 1 month. This allows for the use of MLS data to model the time-of-day dependence of stratospheric temperatures for each lidar location.

Figure 2 shows MLS-minus-NMC 2-mbar temperature differences at Table Mountain Observatory in California, as a function of the time of day of the MLS measurement for spring 1992. We use all MLS version 3, level 3AT data, within a 5° latitude-longitude box of the lidar location. The NMC analysis value over Table Mountain, derived from NOAA 11 data, is always taken at about 0400 LT. MLS data are taken throughout the day, over the season. Thus the MLS-minus-NMC temperature differences in Figure 2 show the dependence of the MLS temperature on the time of day. Subtracting the NMC temperatures from the MLS temperatures eliminates the day-to-day temperature variation, measured by both systems. Also shown in Figure 2 is a fit to the season's data, using a constant term, and sine and cosine terms with 24- and 12-hour periods. This gives a representation of the diurnal and semidiurnal variation of 2-mbar temperature at that location. Results like this were calculated for each lidar location, each pressure level, and each season.

In this study the emphasis is on the ability to fit the MLS versus time-of-day curve, so that a time-of-day adjustment may be made to the lidar data, not on the interpretation of the results as true diurnal and semidiurnal amplitudes. Thus no effort was made to remove the trend from the data, and we do not present the values for the amplitudes and phases here. However, it is important to note that the values are comparable to the expected results. Previous diurnal studies in the 30- to 50-km region include fits to data from the improved stratospheric and mesospheric sounder (ISAMS) on UARS for a 44°N latitude band during December 5, 1991, to January 13, 1992 [*Dudhia et al.*, 1993], and to lidar data at CEL during January 20–31, 1989 [*Gille et al.*, 1991]. Both of these studies and our fits to MLS data for winter 1992 yield diurnal and semidiurnal amplitudes in the range 0.5–4 K, generally increasing with altitude for 10–1 mbar. The details of the altitudinal structure differ in all cases. We also find similar phases to these studies, but we see more structure. We find that the results vary with location, with season, and somewhat with the year of the fit. Since the ISAMS study averages over longitudes, and the lidar study examines 1989 data, we do not expect our results to match those from either study exactly.

To adjust the NMC-versus-lidar comparisons, we calculate the temperature difference of the fitted curve at the times of the NMC and lidar measurements. We use this difference to modify each lidar measurement to the value it is presumed to have at the NMC time, and then proceed to calculate the average NMC-minus-lidar difference for each pressure level and for each location. For instance, in Figure 2 the time of the NMC observation at Table Mountain for levels 5–1 mbar is 1200 UT (0400 LT plus 8 hours difference to UT), and for 10 mbar is also 1200 UT (the time of the radiosonde data). The bulk of lidar data at Table Mountain was taken from 0400 to 0900 UT. For Table Mountain at 2 mbar in the spring

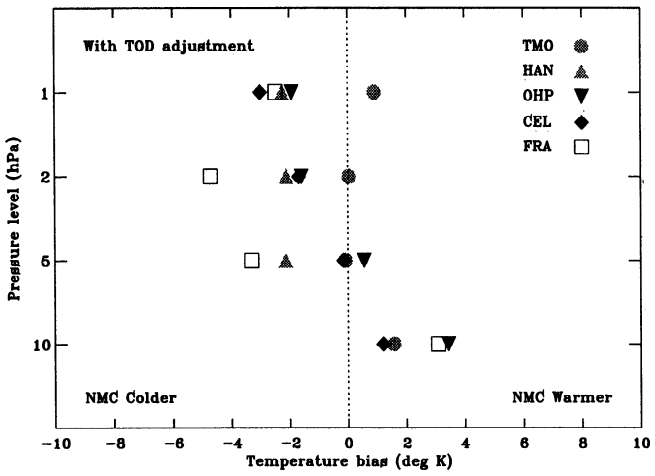

Figure 3. Average stratospheric temperature differences, NMC minus lidar, for the sites as in Figure 1, but including time-of-day (TOD) adjustment. The standard estimate of error is discussed in text.

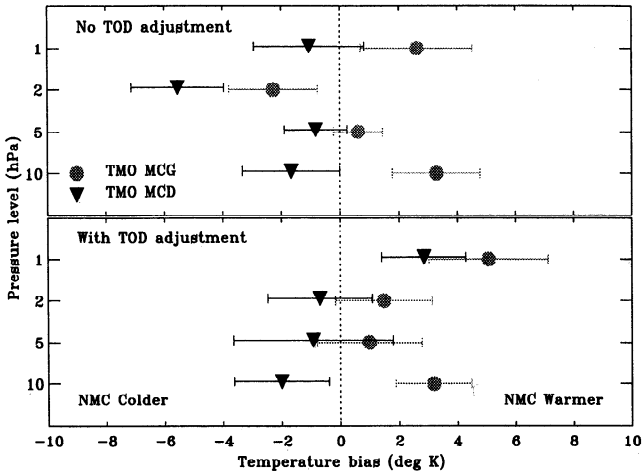

Figure 4. Average stratospheric temperature differences, NMC minus lidar, during the February 19 to March 19, 1992, Table Mountain intercomparison campaign with McGee (MCG) and McDermid (MCD). The bottom graph includes the time-of-day adjustment; the top graph does not. Error bars shown are twice the standard estimate of error.

of 1992, this results in time-of-day adjustments that decrease the lidar temperature by 3–5 K.

Figure 3 shows the time-of-day adjusted NMC-minus-lidar average temperature differences for all the lidar stations, in the same format as in Figure 1. The average differences as found for the European sites have moved to the left, whereas those for the U.S. sites have moved to the right. As a result, there is improvement in the interstation agreement for the French and U.S. stations at all levels. This improvement is summarized in Table 3. As expected, the greatest improvement is at the highest altitude (lowest pressure level), where diurnal effects are largest. The spread of the average temperature differences at different U.S. and French lidar locations, after time-of-day adjustments, ranges from 2.1 to 3.9 K at the various pressure levels.

Small improvements are made to the comparison between CEL and OHP as compared with NMC. The bias reduces from 2.3, 1.7, 0.9, and 1.2 K at 10, 5, 2, and 1 mbar to 2.2, 0.8, 0.1, and 1.1 K.

Like the other European sites, the Frascati points have moved to the left in all cases, though the shift is small even at 1 mbar (0.4 K), where the shift for the French sites is large (3.4 K). The small adjustment for Frascati as compared with OHP is due to the timing of the measurements. For Frascati the times of the NMC and lidar measurements are 1330 UT and 1700–2000 UT, respectively. The associated values on the 1-mbar temperature adjustment curve are roughly equal. For OHP, however, the NMC and lidar times are 1500 UT and 1800–0200 UT, which are at a maximum and minimum on the 1-mbar temperature adjustment curve, indicating a large correction. As a result at 10 and 1 mbar, the Frascati points lie within the U.S.-French cluster, whereas at 5 and 2 mbar, they remain significantly to the left of the averages from the rest of the sites. As Table 3 indicates, there is less agreement after the diurnal adjustment is performed at 5 and 2 mbar with the Frascati points included. Since the confidence of each average difference is 1–2 K, the residual spread of the differences among stations may reflect some unknown effects in the data sets.

Table 3. Scatter of Lidar-NMC Averages

Pressure Level, mbar	No Adjustment, K	With Time-of-Day Adjustment, K	
		With Frascati	Without Frascati
1	6.7	3.9	3.9
2	3.9	4.7	2.1
5	3.7	3.9	2.7
10	3.4	2.2	2.2

Further information about lidar temperature compatibility is available from two special direct intercomparisons of lidar systems. The mobile Goddard Space Flight Center (GSFC) lidar (McGee) was transported to Table Mountain and to OHP for these direct comparisons. (See Table 1 for dates and number of days for each comparison set.) For each of these single-site intercomparisons, the NMC time is the same for the two data sets. The two lasers used in the Table Mountain comparison operate at the same wavelength. For this case, one lidar creates background noise for another. The instruments cannot be operated concurrently, and there exists a few hours difference between lidar measurements from each instrument. For the OHP comparison the lidars use different wavelengths and thus can operate simultaneously. However, time differences of 1 hour are common. Results of comparisons of NMC-minus-lidar average temperature differences are shown in Figures 4 and 5, for Table Mountain and for OHP, respectively. The top graphs in Figures 4 and 5 contain no time-of-day adjustments, and the bottom graphs include the adjustments.

For the Table Mountain comparisons (Figures 4) there is statistically significant disagreement between the two lidar data sets at 1, 2, and 10 mbar, but not at 5 mbar, before diurnal and semidiurnal adjustments are made. When data are adjusted to compensate for the time of day of the measurements, there is moderate improvement. Only at 10 mbar do the lidar data sets significantly disagree.

For OHP (Figure 5) there is good agreement between the

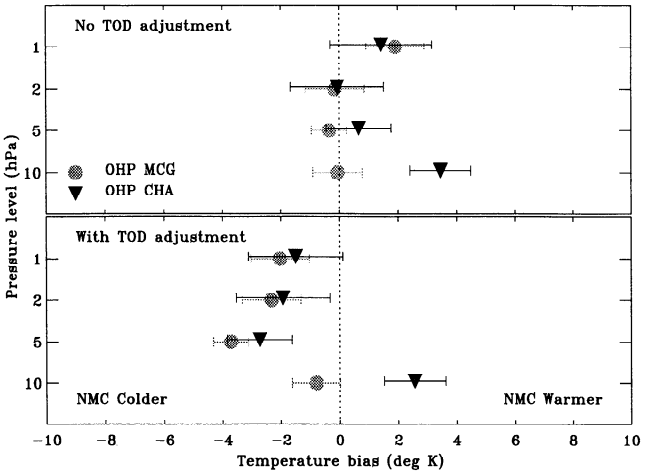

Figure 5. As Figure 4 but for McGee (MCG) and Chanin (CHA) at OHP during July 13 to August 17, 1992.

temperatures of the two lidars at 5, 2, and 1 mbar both before and after time-of-day adjustments are made. At 10 mbar, inclusion of the adjustment does not reduce the 3.4 K disagreement. Since McGee's lidar is here using the Raman channel to retrieve temperature at low altitudes, and since the 532-nm wavelength of the OHP lidar is particularly sensitive to aerosols, the disagreement is possibly due to a Pinatubo-caused aerosol layer near 30 km that would yield too low temperature values for the French Rayleigh lidar.

Discussion

We have shown that diurnal and semidiurnal temperature effects are significant in the 30- to 50-km range. These effects must be included when examining comparisons between lidar and NMC data from global sites. The application of a diurnal and semidiurnal temperature adjustment can shift the yearly average of NMC-lidar temperature differences for a single station by as much as 3.4 K. Since the time of the NMC data in Europe is approximately 1530 LT and in the United States is approximately 0330 LT, the comparison between U.S. and European stations is affected by time-of-day considerations. When we apply a time-of-day adjustment, the resulting agreement between the average NMC-lidar temperature difference for the French and U.S. stations is improved at all levels, but a residual spread of 2–4 K, increasing with altitude, is seen. We consider this an indication of the accuracy of the available operational lidar data in this altitude region. The inclusion of Frascati data degrades the agreement at 5 and 2 mbar to 3.9 and 4.7 K.

Short-term studies comparing two sets of lidar data taken at a single site show that the inclusion of diurnal and semidiurnal effects can make improvements of up to 1 K at the top levels. Time-of-day adjustments yield moderate improvement in the TMO two-lidar comparison for 2 and 1 mbar for which the difference between the lidar measurements improves from 3.7 and 3.2 K to 2.3 and 2.2 K. At 10 and 5 mbar at TMO and at all levels at OHP the change is small. Time-of-day adjustments do not reduce the large disagreement between instruments at a single site at 10 mbar: 3.4 and 5.1 K for OHP and TMO.

Finally, the comparison of NMC analyses at 10 mbar to Rayleigh lidar is hampered by aerosols that tend to make lidar temperatures too cold. This is evidenced by lidars being 1–4 K colder than NMC at this level. A short-term study using Raman lidar for low altitudes at OHP yields statistically insignificant NMC-lidar differences. The brevity of this comparison demands that more work be done before strong conclusions are made. At higher levels, 5–1 mbar, the rocketsonde-adjusted NMC temperature analyses are colder than lidar by 0.5–1.5 K.

References

Adriani, A., G. P. Gobbi, F. Congeduti, and G. Di Donfrancesco, Lidar observations of stratospheric and mesospheric temperature: November 1988–November 1989, *Ann. Geophys.*, *9*, 252–258, 1991.

Cressman, G. P., An operational objective analysis system, *Mon. Weather Rev.*, *87*, 367–374, 1959.

Dao, P. D., W. Klemetti, D. Sipler, W. P. Moskowitz, and G. Davidson, Density measurements with combined Raman-Rayleigh lidar, in *Laser Applications in Meteorology and Earth and Atmospheric Remote Sensing, Proceedings of SPIE, 1062*, edited by M. M. Sokolosky, pp. 138–143, Society of Photo-Optical Instrumentation Engineers, Bellingham, Wash., 1989.

Dao, P. D., J. W. Meriwether, R. McNutt, W. Klemetti, W. Moskowitz, and G. Davidson, Application of lidar to atmospheric sounding of density and temperature, Astrodynamics 1989, *Adv. Astronaut. Sci.*, *71(II)*, 715–726, 1990.

Dudhia, A., S. E. Smith, A. R. Wood, and F. W. Taylor, Diurnal and semi-diurnal temperature variability of the middle atmosphere, as observed by ISAMS, *Geophys. Res. Lett.*, *20*, 1251–1254, 1993.

Ferrare, R. A., et al., Lidar measurements of stratospheric temperature during STOIC, *J. Geophys. Res.*, this issue.

Finger, F. G., H. M. Woolf, and C. E. Anderson, A method for objective analysis of stratospheric constant-pressure charts, *Mon. Weather Rev.*, *93*, 619–638, 1965.

Finger, F. G., M. E. Gelman, J. D. Wild, M. L. Chanin, A. Hauchecorne, and A. J. Miller, Evaluation of NMC upper stratospheric temperature analyses using rocketsonde and lidar data, *Bull. Am. Meteorol. Soc.*, *74*, 789–799, 1993.

Fleming, H. E., M. D. Goldberg, and D. S. Crosby, Minimum variance simultaneous retrieval of temperature and water vapor from satellite radiance measurements, in *Second Conference on Satellite Meteorology/Remote Sensing and Application*, pp. 20–23, American Meteorological Society, Boston, Mass., 1986.

Fleming, H. E., M. D. Goldberg, and D. S. Crosby, Operational implementation of the minimum variance simultaneous method, in *Third Conference on Satellite Meteorology and Oceanography*, pp. 16–19, American Meteorological Society, Boston, Mass., 1988.

Gelman, M. E., K. W. Johnson, and R. M. Nagatani, Detection of long-term trends in global stratospheric temperature from NMC analyses derived from NOAA satellite data, *Adv. Space Res.*, *6*, 17–26, 1986.

Gille, S. T., A. Hauchecorne, and M. L. Chanin, Semidiurnal and diurnal tidal effects in the middle atmosphere as seen by Rayleigh lidar, *J. Geophys. Res.*, *96*, 7579–7587, 1991.

Goldberg, M. D., J. M. Daniels, and H. E. Fleming, A method for obtaining an improved initial approximation for the temperature/moisture retrieval problem, in *Third Conference on Satellite Meteorology and Oceanography*, pp. 20–23, American Meteorological Society, Boston, Mass., 1988.

Hauchecorne, A., and M. L. Chanin, Density and temperature profiles obtained by lidar between 35 and 70 km, *Geophys. Res. Lett.*, *7*, 565–568, 1980.

Hauchecorne, A., M. L. Chanin, and P. Keckhut, Climatology and trends of the middle atmospheric temperature (33–87 km) as seen by Rayleigh lidar over the south of France, *J. Geophys. Res.*, *96*, 15,297–15,309, 1991.

Hauchecorne, A., M. L. Chanin, P. Keckhut, and D. Nedeljkovic, Lidar monitoring of the temperature in the middle and lower atmosphere, *Appl. Phys. B*, *55*, 29–34, 1992.

Keckhut, P., M. L. Chanin, and A. Hauchecorne, Stratospheric

temperature measurement using Raman lidar, *Appl. Opt.*, *29*, 5182–5186, 1990.

Keckhut, P., A. Hauchecorne, and M. L. Chanin, A critical review of the database acquired for the long-term surveillance of the middle atmosphere by the French Rayleigh lidars, *J. Atmos. Oceanic Technol.*, *10*, 850–867, 1993.

Kurylo, M. J., and S. Solomon, Network for the detection of stratospheric change: A status and implementation report, 70 pp., NASA, Washington, D. C., 1990.

McCormick, M. P., *Third International Lidar Researchers Directory*, 181 pp., Atmospheric Sciences Division, NASA Langley Research Center, Hampton, Va., 1993.

McDermid, I. S., Ground-based lidar and atmospheric studies, *Surv. Geophys.*, *9*, 107–122, 1987.

McGee, T. J., U. N. Singh, M. Gross, W. S. Heaps, and R. Ferrare, Lidar measurements of stratospheric ozone, temperature and aerosol during 1992 UARS correlative measurement campaign, in Proceedings of 16th International Laser Radar Conference, *NASA Conf. Publ.*, *CP 3158*, Part 1, 103–105, 1992.

Measures, R. M., *Laser Remote Sensing: Fundamentals and Applications*, 510 pp., John Wiley, New York, 1984.

Nedeljkovic, D., A. Hauchecorne, and M. L. Chanin, Rotational Raman lidar to measure the atmospheric temperature from ground to 30 km, *IEEE Trans. Geosci. Remote Sens.*, *31*, 90–101, 1993.

Waters, J. W., Microwave limb sounding, in *Atmospheric Remote Sensing by Microwave Radiometry*, edited by M. A. Janssen, pp. 383–496, John Wiley, New York, 1993.

A. Adriani, F. Congeduti, and G. P. Gobbi, Istituto di Fisica dell'Atmosfera, CNR, Via G. Galilei-C. P. 27, 00044 Frascati, Italy.

M. L. Chanin, A. Hauchecorne, and P. Keckhut, Service d'Aeronomie de Centre National de la Recherche Scientifique, BP 3, 91371 Verrieres le Buisson, France.

P. D. Dao and R. Farley, Air Force Phillips Laboratory, Geophysics Directorate, Hanscom AFB, Bedford, MA 01731.

E. F. Fishbein, Jet Propulsion Laboratory, California Institute of Technology, Pasadena, CA 91109.

M. E. Gelman, A. J. Miller, and J. D. Wild, Climate Analysis Center, NMC, NWS, NOAA, Washington, DC 20233.

I. S. McDermid, Jet Propulsion Laboratory, P.O. Box 367, Table Mountain Facility, Wrightwood, CA 92397-0367.

T. J. McGee, Laboratory for Atmospheres, NASA Goddard Space Flight Center, Greenbelt, MD 20771.

J. W. Meriwether, Department of Physics and Astronomy, University of Clemson, Clemson, SC 29634-1911.

(Received August 2, 1994; revised February 10, 1995; accepted February 11, 1995.)